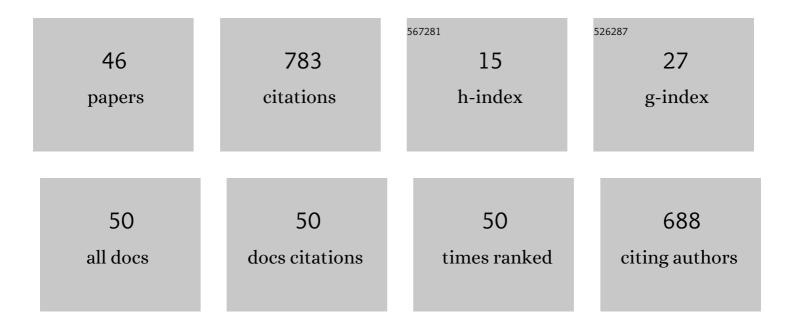
Da-Chuan Cheng

List of Publications by Year in descending order

Source: https://exaly.com/author-pdf/1416053/publications.pdf Version: 2024-02-01



#	Article	IF	CITATIONS
1	Modeling the Enhanced Efficacy and Curing Depth of Photo-Thermal Dual Polymerization in Metal (Fe) Polymer Composites for 3D Printing. Polymers, 2022, 14, 1158.	4.5	1
2	Prediction of All-Cause Mortality Based on Stress/Rest Myocardial Perfusion Imaging (MPI) Using Deep Learning: A Comparison between Image and Frequency Spectra as Input. Journal of Personalized Medicine, 2022, 12, 1105.	2.5	0
3	Lesion-Based Bone Metastasis Detection in Chest Bone Scintigraphy Images of Prostate Cancer Patients Using Pre-Train, Negative Mining, and Deep Learning. Diagnostics, 2021, 11, 518.	2.6	27
4	Bone Metastasis Detection in the Chest and Pelvis from a Whole-Body Bone Scan Using Deep Learning and a Small Dataset. Electronics (Switzerland), 2021, 10, 1201.	3.1	20
5	A Critical Review for Synergic Kinetics and Strategies for Enhanced Photopolymerizations for 3D-Printing and Additive Manufacturing. Polymers, 2021, 13, 2325.	4.5	14
6	Enhancing blue-light-initiated photopolymerization in a three-component system: kinetic and modeling of conversion strategies. Journal of Polymer Research, 2021, 28, 1.	2.4	10
7	Enhancing UV Photopolymerization by a Redâ€light Preirradiation: Kinetics and Modeling Strategies for Reduced Oxygen Inhibition. Journal of Polymer Science, 2020, 58, 683-691.	3.8	11
8	Organ Contouring for Lung Cancer Patients with a Seed Generation Scheme and Random Walks. Sensors, 2020, 20, 4823.	3.8	3
9	3-Wavelength (UV, Blue, Red) Controlled Photo-Confinement for 3D-Printing: Kinetics and Modeling. IEEE Access, 2020, 8, 49353-49362.	4.2	8
10	Dual-Function Enhancer for Near-Infrared Photopolymerization: Kinetic Modeling for Improved Efficacy by Suppressed Oxygen Inhibition. IEEE Access, 2020, 8, 83465-83471.	4.2	5
11	Systematic Quantification of Cell Confluence in Human Normal Oral Fibroblasts. Applied Sciences (Switzerland), 2020, 10, 9146.	2.5	4
12	Dual-Wavelength (UV and Blue) Controlled Photopolymerization Confinement for 3D-Printing: Modeling and Analysis of Measurements. Polymers, 2019, 11, 1819.	4.5	20
13	Modeling the Kinetics, Curing Depth, and Efficacy of Radical-Mediated Photopolymerization: The Role of Oxygen Inhibition, Viscosity, and Dynamic Light Intensity. Frontiers in Chemistry, 2019, 7, 760.	3.6	40
14	Thiol–Ene Photopolymerization: Scaling Law and Analytical Formulas for Conversion Based on Kinetic Rate and Thiol–Ene Molar Ratio. Polymers, 2019, 11, 1640.	4.5	13
15	Noninvasive assessment of intracranial elastance and pressure in spontaneous intracranial hypotension by MRI. Journal of Magnetic Resonance Imaging, 2018, 48, 1255-1263.	3.4	8
16	Computer-assisted system on mandibular canal detection. Biomedizinische Technik, 2017, 62, 575-580.	0.8	2
17	ADAM9 promotes lung cancer progression through vascular remodeling by VEGFA, ANGPT2, and PLAT. Scientific Reports, 2017, 7, 15108.	3.3	37
18	Using impedance-plethysmography technique for cuffless blood pressure measurement. , 2017, , .		2

DA-CHUAN CHENG

#	Article	IF	CITATIONS
19	A Cuffless Blood Pressure Measurement Based on the Impedance Plethysmography Technique. Sensors, 2017, 17, 1176.	3.8	40
20	Modeling the efficacy profiles of UV-light activated corneal collagen crosslinking. PLoS ONE, 2017, 12, e0175002.	2.5	34
21	Elliptic Shape Prior Dynamic Programming for Accurate Vessel Segmentation in MRI Sequences with Automated Optimal Parameter Selection. Journal of Medical and Biological Engineering, 2016, 36, 651-660.	1.8	2
22	Assessment of the endothelial function with changed volume of brachial artery by menstrual cycle. BioMedical Engineering OnLine, 2016, 15, 106.	2.7	5
23	Accurate Measurement of Cross-Sectional Area of Femoral Artery on MRI Sequences of Transcontinental Ultramarathon Runners Using Optimal Parameters Selection. Journal of Medical Systems, 2016, 40, 260.	3.6	3
24	Assessment of Stroke Volume From Brachial Blood Pressure Using Arterial Characteristics. IEEE Transactions on Biomedical Engineering, 2015, 62, 2151-2157.	4.2	13
25	Optimal Focusing and Scaling Law for Uniform Photo-Polymerization in a Thick Medium Using a Focused UV Laser. Polymers, 2014, 6, 552-564.	4.5	13
26	Modeling the Kinetics of Enhanced Photo-Polymerization under a Collimated and a Reflecting Focused UV Laser. Polymers, 2014, 6, 1489-1501.	4.5	7
27	The Progression of Muscle Fatigue During Exercise Estimation With the Aid of High-Frequency Component Parameters Derived From Ensemble Empirical Mode Decomposition. IEEE Journal of Biomedical and Health Informatics, 2014, 18, 1647-1658.	6.3	17
28	Automated Feature Set Selection and Its Application to MCC Identification in Digital Mammograms for Breast Cancer Detection. Sensors, 2013, 13, 4855-4875.	3.8	9
29	Arrhythmia Identification with Two-Lead Electrocardiograms Using Artificial Neural Networks and Support Vector Machines for a Portable ECG Monitor System. Sensors, 2013, 13, 813-828.	3.8	30
30	Automated localisation and boundary identification of superficial femoral artery on MRI sequences. Computer Methods in Biomechanics and Biomedical Engineering, 2013, 16, 873-884.	1.6	3
31	Title is missing!. Journal of Medical and Biological Engineering, 2013, 33, 486.	1.8	4
32	Analysis of Scaling Law and Figure of Merit of Fiber-Based Biosensor. Journal of Nanomaterials, 2012, 2012, 1-7.	2.7	6
33	Three-Dimensional Expansion of a Dynamic Programming Method for Boundary Detection and Its Application to Sequential Magnetic Resonance Imaging (MRI). Sensors, 2012, 12, 5195-5211.	3.8	11
34	Automatic detection of the carotid artery boundary on cross-sectional MR image sequences using a circle model guided dynamic programming. BioMedical Engineering OnLine, 2011, 10, 26.	2.7	17
35	AUTOMATIC DETECTION OF COLORECTAL POLYPS IN STATIC IMAGES. Biomedical Engineering - Applications, Basis and Communications, 2011, 23, 357-367.	0.6	10
36	ESTIMATING THE MEAN BLOOD FLOW OF ARM BASED ON WINDKESSEL MODEL. Biomedical Engineering - Applications, Basis and Communications, 2011, 23, 349-356.	0.6	2

DA-CHUAN CHENG

#	Article	IF	CITATIONS
37	Automated Detection of the Arterial Inner Walls of the Common Carotid Artery Based on Dynamic B-Mode Signals. Sensors, 2010, 10, 10601-10619.	3.8	14
38	Non-invasive determination of instantaneous brachial blood flow using the oscillometric method. Biomedizinische Technik, 2009, 54, 171-177.	0.8	2
39	Improved Arterial Inner Wall Detection Using Generalized Median Computation. Lecture Notes in Computer Science, 2009, , 622-630.	1.3	0
40	Detections of Arterial Wall in Sonographic Artery Images Using Dual Dynamic Programming. IEEE Transactions on Information Technology in Biomedicine, 2008, 12, 792-799.	3.2	59
41	Colorectal Polyps Detection Using Texture Features and Support Vector Machine. Lecture Notes in Computer Science, 2008, , 62-72.	1.3	25
42	Quantitative measurement of carotid intima-media roughness—effect of age and manifest coronary artery disease. Atherosclerosis, 2003, 166, 57-65.	0.8	36
43	Quantification of the Wall Inhomogeneity in B-mode Sonographic Images of the Carotid Artery. Journal of Ultrasound in Medicine, 2002, 21, 1395-1404.	1.7	10
44	Using snakes to detect the intimal and adventitial layers of the common carotid artery wall in sonographic images. Computer Methods and Programs in Biomedicine, 2002, 67, 27-37.	4.7	146
45	Computerized analysing system using the active contour in ultrasound measurement of carotid artery intima-media thickness. Clinical Physiology, 2001, 21, 561-569.	0.7	39
46	A PC-based medical image analysis system for brain CT hemorrhage area extraction. , 0, , .		0

A PC-based medical image analysis system for brain CT hemorrhage area extraction. , 0, , . 46